Journal of Materials Chemistry B

Hierarchically macroporous / mesoporous POC composite scaffolds with IBU-loaded hollow SiO2 microspheres for repairing infected bone defects

Journal:	*Journal of Materials Chemistry B*
Manuscript ID	TB-ART-02-2016-000435.R1
Article Type:	Paper
Date Submitted by the Author:	03-May-2016
Complete List of Authors:	Chen, Fangping; East University of Science and Technology, Song, Zhiyan; East China University of Science and Technology, Gao, Li; East China University of Science and Technology Hong, Hua; Engineering Research Centre for Biomedical Materials of Ministry of Education, East China University of Science and Technology, Liu, Changsheng; East China University of Science and Technology

Journal of
Materials Chemistry B

Cite this: DOI: 10.1039/c0xx00000x

www.rsc.org/xxxxxx

ARTICLE TYPE

Hierarchically macroporous / mesoporous POC composite scaffolds with IBU-loaded hollow SiO_2 microspheres for repairing infected bone defects

Fangping Chen*[a, b,c], Zhiyan Song[Δa,c], Li Gao[Δ a,b], Hua Hong[a,b] and Changsheng Liu*[a,b]

Received (in XXX, XXX) XthXXXXXXXXX 20XX, Accepted Xth XXXXXXXXX 20XX
DOI: 10.1039/b000000x

Infected bone defects are normally regarded as contraindications for bone repair. In the present study, a hollow mesoporous structure of silica (SiO_2) microspheres was first synthesized and loaded with Ibuprofen (IBU). Poly(1,8-octanediol-co-citrate)(POC) and β-tricalcium phosphate (β-$Ca_3(PO_4)_2$, β-TCP), together with IBU-loaded SiO_2 were fabricated by 3D printing technique based on Freeform Fabrication System with Micro-Droplet Jetting (FFS-MDJ). The physiochemical properties, compressive modulus, drug release behavior, antimicrobial properties and cell response of the composite scaffold were systematically investigated. The developed IBU-loaded SiO_2/β-TCP/POC scaffolds presented highly interconnected porous network, macropores (350-450 μm) and mesopores (3.65nm), as well as proper compressive modulus and biocompatibility. The addition of hollow SiO_2 microspheres was found to decrease the burst release and increase the cumulative release amount of IBU. In addition, the IBU-loaded SiO_2/β-TCP/POC showed a long-term effect on inhibiting *E. coli* growth by agar diffusion. The result indicated that the IBU-loaded SiO_2/β-TCP/POC scaffold, with hierarchically macro/mesoporous, highly interconnected pore structure and effective antimicrobial property, demonstrates promise for bone regeneration in clinical case of infected bone defects.

Introduction

Bone defect-related infections, especially in open bone trauma and fracture, seriously affect bone union and are regarded as contraindications for bone repair. Therefore, it is necessary to develop biomaterials which can promote reconstruction of bone defects and synchronously inhibit related infections.

Calcium phosphate (CaP) especially beta-tricalcium phosphate (β-TCP) is the material of first choice since its composition is similar to the natural bone and as such has required a hydrophilic bioceramic, which has osteoconductive and biodegradable

[a]*The State Key Laboratory of Bioreactor Engineering, East China University of Science and Technology, Shanghai 200237, PR China.Fax: 86-21-64251358; Tel.:86-21-64251308; E-mail:fpchen@ecust.edu.cn*

[b]*Key Laboratory for Ultrafine Materials of Ministry of Education, School of Materials Science and Engineering, East China University of Science and Technology, Shanghai 200237, PR China*

[c]*Shanghai Collaborative Innovation Center for Biomanufacturing, East China University of Science and Technology, Shanghai 200237, PR China*

Δ *The two authors contributed equally.*

*Email of corresponding author : fpchen@ecust.edu.cn ; csliu@sh163.net

properties.[1]However, the intrinsic brittleness and lack processability is generally encountered in the current β-TCP based scaffolds, which hampers their applications, especially in repairing the load-bearing bone defect. One alternative to overcome this hurdle is offered by a ceramic-polymer composite biomaterial, which incorporates the desirable properties of each of the constituent materials. Poly(1,8-octanediol-co-citrate) (POC), a covalently cross-linked elastomer based on the polymerization of citric acid and 1,8-octanediol, has been widely explored in the field of tissue repair.[2,3]Compared with other synthetic biodegradable polymers, POC exhibits super elastic stretch ability similar to the mechanical character of biological tissues. More importantly, the mechanical strength and degradation rate of POC can be controlled by synthetic conditions of the polycondensation reaction. In addition, POC and its degradation product are biocompatible without the addition of initiators. Inspired by these excellent properties associated with POC, we hypothesize that addition of POC pre-polymers into β-TCP to improve the robustness and processability of brittle β-TCP scaffolds. [4]

Since the functionality of bone tissues is related with their complex architecture, tissue scaffolds have been trying to mimic this complexity.It is necessary for a bone scaffold to possess sufficient porosity, pore dimension and pore interconnectivity for proper oxygen/nutrient delivery, directing cell fate and tissue ingrowth [5]. A three-dimensional (3D) printing is a relatively recent phenomenon, and this research field is under intense exploration[6]. Freeform Fabrication System with Micro-Droplet Jetting (FFS-MDJ), one of 3D print methods, was used to fabricate scaffolds with materials acting as the “ink”. Controllable pore shapes and complex structures can be created by FFS-MDJ, facilitating high diffusion of nutrients and metabolites required for tissue regeneration [7-9]. Therefore, β-TCP/POC scaffolds are printed by FFS-MDJ in this study to obtain the connected pore structures.

The scaffolds for bone treatment always associated with the occurrence of infections because of the easiness of microbial attack at sites where it is open area to environment[10]. Anti-inflammatory drugs tend to be loaded in the scaffold by adsorption, and play pivotal roles in preventing the bone infection. While a combination of composite scaffolds and drugs is deemed to be promising, one challenge lies in accomplishing a controlled release of drugs in scaffolds to meet intrinsic needs of long term resistance to bacteria and tissue regeneration.[11-12] So far, a consensus on an optimal release profile of drugs has not been achieved yet. Before drugs loading in scaffolds, the addition of drugs in microspheres can carry more drug and effectively decrease burst release. [13-15] Hollow mesoporous silica spheres have been well developed as a drug carrier with excellent controllable release, nontoxicity, good stability and biocompatibility. [16-18]

Therefore, in this study, novel composite scaffolds composed of β-TCP, POC and drug-loaded mesoporous silica spheres were printed directly by FFS-MDJ after the drug was loaded in the hollow silica microspheres. The morphological characteristics, mechanical property, cell compatibility, drug release behavior and their antibacterial effect against E. coli were investigated. Ibuprofen (IBU) was chosen as the drug with an anti-inflammatory and analgesic effect. We hypothesize that the POC composite scaffolds with IBU-loaded hollow SiO_2 microsphere may greatly improve the osteogenic and antimicrobial properties by virtue of their interconnected pore structure and controllable release.

Experimental

Preparation and characterization of pre-POC and IBU-loaded SiO_2 microspheres

POC pre-polymer was synthesized via a two-step condensation polymerization as previously described.[19-20] Briefly, an equimolar mixture of citric acid and 1,8-octanediol were melted in a three-neck round-bottom flask at 140 °C under argon atmosphere for 36 h. After reducing the vacuum pressure from 1 Torr to 50 m Torr over 2 h, further polymerization continued for 6 h at 160 °C. The obtained viscous mixture was dissolved in ethanol and precipitated in water. The precipitate was further purified by dialysis membrane (COMW 10,000 Da, Shanghai Yuan Ju Biological Technology Co., Ltd., China) for 24 h, followed by lyophilization to get the POC pre-polymer . β-TCP was prepared by a modified wet chemical precipitation method with calciumhydroxide ($Ca(OH)_2$) and orthophosphoric acid (H_3PO_4) solution.[21]

Hollow silicon dioxide (SiO_2) spheres were synthesized as previously described. [22] 71.6 ml of ethanol, 10 ml deionized water and 3.14 ml ammonia were mixed by stirring at 30 °C for 30 min. 6ml tetraethylorthosilicate (TEOS) was then added rapidly and stirred for 40 min. A mixture of 5ml TEOS and 2ml N-(2-aminoethyl) 3-aminopropyltrimetyoxysilane was added and magnetically stirred for another 80 min. After separated by centrifugalization, the SiO_2 microspheres were dispersed in sodium carbonate to etch for 60 min, washed by deionized water for three times and then freeze dried. Disperse 50 mg hollow SiO_2 microspheres in 50 mg/mL IBU/ethanol solution and stirred for 48 h. IBU loaded hollow SiO_2 microspheres were obtained after centrifuge and freeze drying.

The morphology of SiO_2 microspheres was visualized with Transmission electron microscopy (TEM, JEM-1400F, JEOL, Japan). Nitrogen adsorption-desorption isotherms at 77K for SiO_2 microspheres was measured on a Micrometitics Tristar 3000 system. The pore size distributions, pore volume and specific surface area were calculated by the Barrett Joyner Halenda (BJH) and Langmuir methods, respectively. Infrared spectra were recorded with Fourier transformation infrared (FTIR, Nicolet 5700, Thermo Ltd, USA) spectrometer within the wavelength range of 4000 - 400 cm^{-1}. The phase composition of SiO_2 and IBU-loaded SiO_2 were verified by X-ray diffraction (XRD, D/Max-2550 V diffractometer, Rigaku, Japan).

Preparation of IBU-loaded SiO_2/β-TCP/POC and pure IBU/β-TCP/POC scaffold

β-TCP powders were grinded with pot mill and sieved with a 400 mesh sieve. Pre-POC was dissolved in ethanol to form a homogeneous solution and mixed with IBU-loaded SiO_2 and β-TCP at room temperature by continuous stirring. The pre-POC ethonal solution was used as a binder. Paste was prepared to be printable by mixing the pre-POC, IBU-loaded hollow SiO_2 microsphere and β-TCP according to the weight ratios listed in table 1.

The printable paste was first fed into the stainless steel syringe of FFS-MDJ at room temperature, and then extruded through the small nozzle with an inner diameter of 510 μm. The scaffold was printed layer by layer according to the predefined pattern with a layer thickness of 0.9 mm. The architecture of IBU-loadedSiO_2/β-TCP/POC scaffolds were changed by extruding pastes with -45° and 45° angles for every other layer. Finally, the complex scaffolds were formed by post-polymerizing at 80 °C for 3 days. Pure IBU/β-TCP/POC scaffold was printed the same as the IBU loaded SiO_2/β-TCP/POC except that the same amount of IBU was directly mixed with pre-POC.

Characterization of SiO_2/β-TCP/POC composite scaffolds

The surface morphology of the composite scaffold was observed by scanning electron microscope (SEM, H-800, Hitachi, Japan) at a high magnification with an acceleration voltage of 15 kV. FTIR spectra was obtained from KBr pellets at wavelengths ranging from 4000 to 400 cm^{-1} at a resolution of 1 $cm^{-1}$with an average of 64 scans. The elements of the samples were confirmed by energy dispersive spectroscopy (EDS).

Table 1. Compositions and printing parameters of POC composite scaffolds

Samples	POC (wt%)	β-TCP (wt%)	IBU-loaded SiO_2 (wt%)	Nozzle diameter (mm)	Interspacing distance (mm)
SiO_2/β-TCP/POC	42.5	55	2.5	0.51	0.39
β-TCP/POC	45	55	0	0.51	0.39

The mechanical property of the IBU-loaded SiO_2/β-TCP/POC and β-TCP/POC scaffolds (10×10×10 mm) was measured with a universal testing machine (INSTRON Ltd., USA). The loading rate was 1mm/min the direction perpendicular to the compressive plane. Three replicates were carried out for each group.

Assessment of IBU release in vitro and antibacterial properties

Scaffolds with IBU-loaded SiO_2 and pure IBU (10×10×2 mm) were incubated at 37 °C in PBS (0.01M, pH =7.2) under agitation with 80 rpm stirring. After specified time intervals, 5 mL of the supernatant was collected and an equal amount of fresh PBS was added. The amount of released IBU was determined by measuring the absorbance at 220 nm on a UV-vis spectrophotometer (Spectra Max M2, Molecular, USA). The release profiles were obtained by plotting the percentage of cumulatively released IBU contents against time. Each experiment was performed in triplicate.

The antimicrobial properties of the IBU-loaded SiO_2/β-TCP/POC and β-TCP/POC were tested by agar diffusion using *E. coli* (diameter of 10 mm, height of 5 mm) of each scaffold were printed by FFS-MDJ. The scaffolds were allowed to set at 37 °C and 90% relative humidity for 4 h. The bacterial strain was maintained as subcultures on trypticase soy agar (TSA) plates supplemented with 5% defibrinated sheep blood at 37 °C in a 5% CO_2 atmosphere. As the antimicrobial activity of the scaffolds results from drug diffusion into the agar gel, a uniform gel thickness of 2 mm was maintained. The bacteria (10 μL) were cultivated in 2 mL of TSA medium for 24 h at 37 °C. Subsequently the culture was diluted (1:4) with water, and 50 mL of this suspension was homogeneously dispersed on each agar plate. The scaffold was placed at the center of the agar plate, and the inhibition zone around the scaffold was measured after 1, 6, and 18 days of incubation at 37 °C. Three samples of each scaffold were tested.

Cell viability of IBU-loaded SiO_2/β-TCP/POC scaffolds

Cell viability was evaluated by a methyl thiazolyl tetrazolium (MTT) assay. [23] In brief, SiO_2/β-TCP/POC and IBU-loaded SiO_2/β-TCP/POC scaffolds were first put in each well of the 24-well culture plate. C2C12 cells, a myoblastic precursor cell with osteoblastic potential, were then seeded onto the scaffolds at a density of 2×10^4 cells per well, followed by static incubation at 37 °C and 100 % humidity with 5 % CO_2 in Dulbecco's modified Eagle's medium–bovine fetal serum (DMEM). The medium was changed every 2 days. After culturing for 1, 3 and 5 days, 30 μL MTT solution was added to each medium. The plate was then incubated for further 4 h. The supernatant from each well was then removed and 200μL of dimethyl sulfoxide was added. After shaking for 10 min, the optical density (OD) of the chromophore was measured at 492 nm using an enzyme-linked immunoadsorbent assay plate reader (Spectra Max M2, Molecular Devices, USA). Cells cultured directly on 24-well plate were used as control. After culturing for 1d, 3d and 5d in direct contact with the samples and treated by Giemsa staining, the morphology of cells were observed and photographed under a phase contrast microscope (Olympus, Tokyo, Japan).

To further study the cell viability, scaffolds were placed in a 24-well cell culture plate. SiO_2/β-TCP/POC was leached by soaking in culture medium for 24 h. C2C12 cells were seeded with the leach liquor of SiO_2/β-TCP/POC at a density of 1.2×10^5 cells per well. After 24 h incubation, samples were washed with PBS and fixed with formalin solution (3.7% in PBS) for 15 min. The fixed cells were washed with PBS three times, and then stained with FITC-Phalloidin (Sigma, St. Louis, USA) for 30 min. 2-(4-Amidinophenyl)-6-indolecarbamidine dihydrochloride (DAPI, Beyotime Biotech, Jiangsu, China) solution was added to stain cell nuclei for 10 min. The cell morphology was recorded using confocal laser scanning microscopy (LEICA TCS SD_2,

Germany). [24]

Statistical analysis

Statistical analysis was conducted using one-way ANOVA with post hoc tests. The results were expressed as the mean ± standard deviation. A value of $p<0.05$ was considered to be statistically significant.

Results

Characterization of hollow SiO_2 microspheres and IBU-loaded hollow SiO_2 microspheres

An XRD pattern of the obtained samples was shown in Figure 1a. The diffraction peak of the hollow SiO_2 microsphere was broad. Although the main broad peak at approximately 23.8° (2Θ) was consistent with SiO_2 (PDF#29-0085) according to JCPDS crystallographic database, it was considered to be amorphous. TEM image revealed the SiO_2 microsphere was hollow due to alkaline etching. The micrograph showed that the microsphere dispersed well and had a uniform size of approximately 300 nm (Figure 1b).

The pore structural evolution of the hollow SiO_2 spheres was characterized by nitrogen adsorption-desorption technique. The nitrogen adsorption–desorption isotherm of the hollow SiO_2 spheres in Figure 1c shows an adsorption at low pressures, an increase in adsorption with increasing pressure and hysteresis upon desorption. These isotherm characteristics reflect type IV isotherms typical for mesoporous materials. Corresponding to the nitrogen adsorption–desorption isotherm, the BJH adsorption shows the distribution of pore volume and pore diameter, and it can be calculated from the plots, where the specific surface area and mean pore volume of SiO_2 spheres were 293 m^2/g and 0.354 cm^3/g , respectively. The pore size distribution of SiO_2 spheres is narrow (Figure 1d), indicating that the materials had a well-defined mesoporous structure, and the pores were homogeneous and about 3.65 nm.

The chemical structures of IBU-loaded hollow SiO_2 microsphere are characterized by FTIR in Figure 2. The characteristic band at 1720 cm^{-1} was assigned to the stretching vibration of carboxyl groups, which were found in the spectra of the IBU-loaded SiO_2 microsphere while not found in pure SiO_2 microsphere. In fact, the chemical name of IBU is 2 - methyl - 4 - (2 - methyl propyl) benzene acetic acid and contains carboxyl

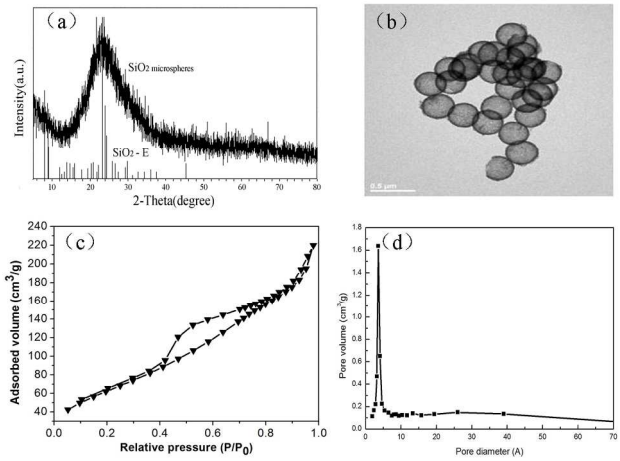

Figure 1.XRD pattern (a), TEM image (b) and N_2 absorption-desorption isotherms (c) and pore diameter distribution (d) of hollow SiO_2 microsphere. *SiO_2-E represents the standard XRD pattern of SiO_2 from the JCPDS crystallographic database

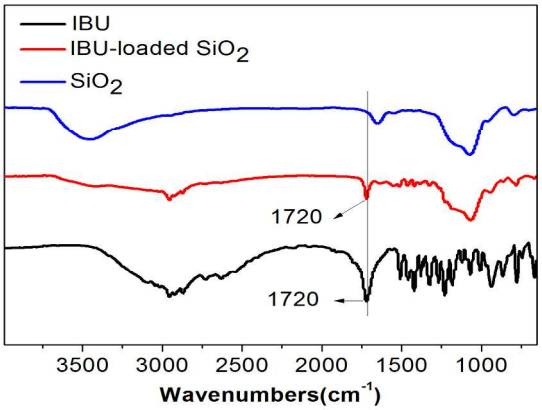

Figure 2. FTIR spectra of IBU-loaded hollow SiO_2 microspheres

groups. The result showed that IBU was successfully loaded into the hollow SiO_2 microspheres.

Figure 3 displays the phase compositions of pure SiO_2, IBU-loaded SiO_2 and IBU. It is obvious to find that the characteristic diffraction peaks of IBU and IBU-loaded SiO_2 were coincident. The XRD result further confirmed that IBU was successfully loaded into the hollow SiO_2 microspheres.

Characterization of SiO_2/β-TCP/POC scaffold

The IBU-loaded SiO_2/β-TCP/POC paste was extruded continuously and homogeneously *via* FFS-MDJ. Figure 4 illustrates the architectures and pore structures of IBU-loaded SiO_2/β-TCP/POC scaffolds. The inner pore shape of the IBU-loaded SiO_2/β-TCP/POC scaffold was changed with the angle of the process pattern. The macrospore size was approximately 350–450μm (Figure 4b) , which is coincidence with the predefined 3D printing parameter. It was clear to see that the pores in the scaffold were uniform and completely open. Tight bonding between different layers was observed in all scaffolds. The result

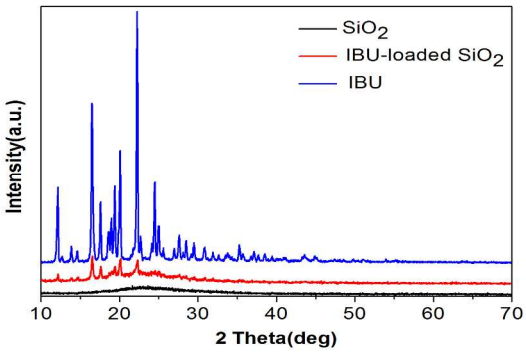

Figure 3. XRD pattern of IBU-loaded hollow SiO_2 microspheres

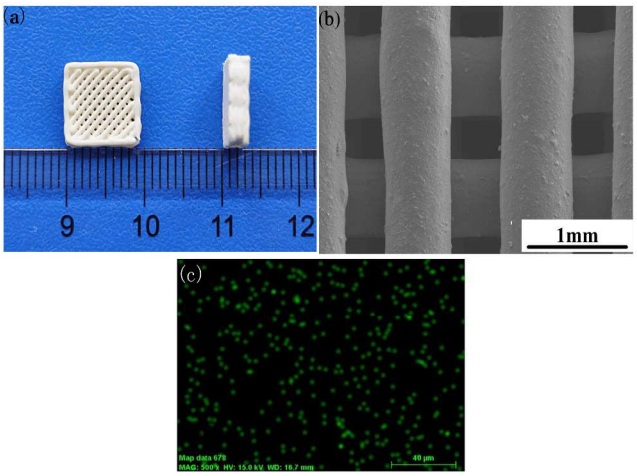

Figure 4. Digital photo (a), SEM image (b) and EDS (c) of Si in SiO_2/β-TCP/POC scaffold

also indicated that the introduction of IBU-loaded SiO_2 microsphere didn't affect the printability and formability of the scaffold.

Figure 4c showed the EDS qualitative assay of silicon in SiO_2/β-TCP/POC scaffolds. It is obvious to see that the green highlight distributed uniformly, indicating that the homogeneous distribution of hollow SiO_2 microspheres in POC composite scaffolds.

Figure 5 displayed the FTIR spectrum of IBU-loaded SiO_2/β-TCP/POC scaffold and β-TCP/POC scaffold. Compared with the spectra of β-TCP/POC, obvious Si-O absorption peaks were found in the IBU-loaded SiO_2/β-TCP/POC scaffold. Except that, there is no difference between the FTIR spectra of two scaffolds. The result indicated that the addition of the hollow SiO_2 microsphere did not react with the other compositions in the scaffold.

Mechanical properties of SiO_2/β-TCP/POC scaffold

Figure 6 plots the mechanical properties of SiO_2/β-TCP/POC scaffold and β-TCP/POC scaffolds. Compared with pure β-TCP/POC scaffold, SiO_2/β-TCP/POC scaffold had higher compressive modulus of 52.29 ± 5.15 MPa.

Assessment of the IBU release and antibacterial properties

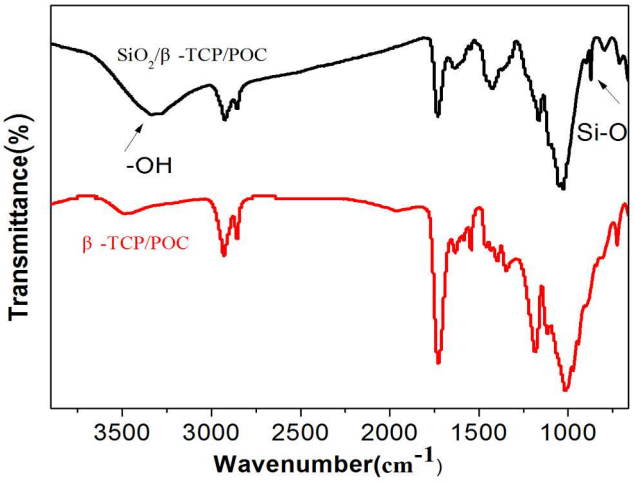

Figure 5. FTIR spectra of IBU-loaded SiO_2/β-TCP/POC and β-TCP/POC scaffolds

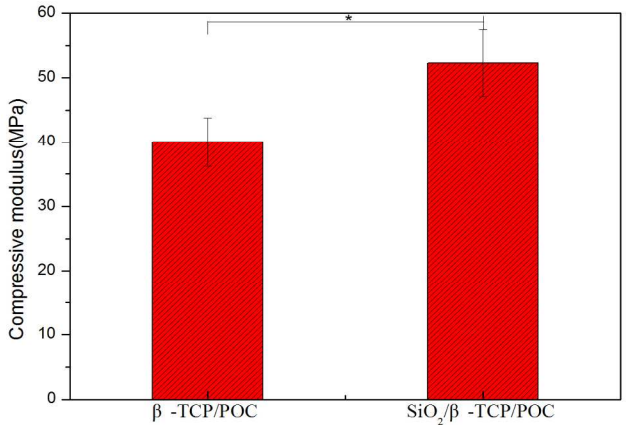

Figure 6. Compressive modulus of POC composite scaffolds

Figure 7 shows the percentage cumulative release of IBU released into the PBS from the β-TCP/POC and SiO_2/β-TCP/POC scaffolds with the time. A burst release at the early stage was observed in the IBU loaded β-TCP/POC while a not-so-obvious release in SiO_2/β-TCP/POC. 22.63 % IBU was released from the β-TCP/POC scaffold after one day, and the amount of IBU reached 47.96 % after 35 days' release. The release rate of IBU from SiO_2/β-TCP/POC scaffold was slower than that from β-TCP/POC scaffolds. The amount of IBU was released 11.40 % after one day and reached 53.69 % after 35 days. In addition, the cumulative release of IBU from β-TCP/POC scaffold was lower than that from SiO_2/β-TCP/POC scaffold. Therefore, the result indicated that the release behavior of IBU was mainly controlled by the SiO_2 spheres because the loaded IBU amount and processing parameters were the same for two scaffolds.

The inhibition ring diameters of SiO_2/β-TCP/POC and β-TCP/POC for *E. coli* culture are listed in Table 2.The inhibition ring diameter increased with the increase of the culture time, indicating that IBU inhibited the growth of *E. coli* no matter it was loaded in hollow SiO_2 microspheres or not. At the first day culture, the inhibition ring diameter of β-TCP/POC was bigger

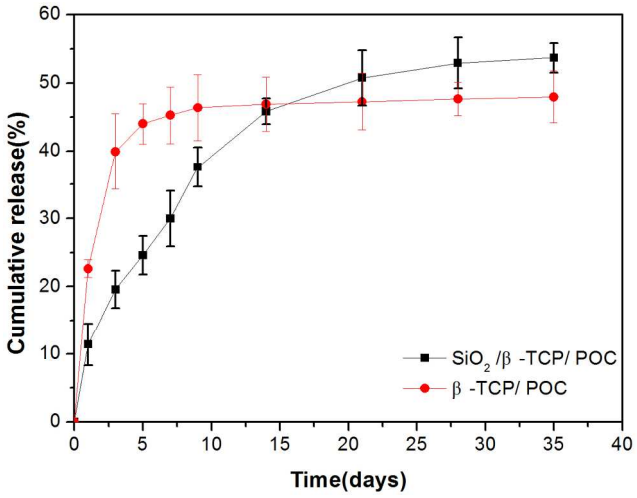

Figure 7.Cumulative release in *vitro* of IBU from SiO_2/β-TCP/POC and β-TCP/POC

than that of SiO_2/β-TCP/POC, revealing that IBU released more rapidly from β-TCP/POC than from SiO_2/β-TCP/POC. After culturing for 6 days, no statistically significant differences were found between the two scaffolds. However, the inhibition zones of SiO_2/β-TCP/POC were significantly larger than that of β-TCP/POC at the 18th day' culture. The result revealed that SiO_2/β-TCP/POC prolonged the IBU release and had a potential long-term antimicrobial effect.

Cell responses to the scaffolds

Figure 8 shows that the viability of C2C12 cells on SiO_2/β-TCP/POC scaffolds increased over the whole culture period by MTT assay. The OD value for SiO_2/β-TCP/POC was significantly higher than that of the control group at 5 days; there was no significant difference at 1 day and 3 days. The result suggested that the SiO_2/β-TCP/POC scaffold facilitate cells growth and promote cell proliferation.

The morphological feature of C2C12 cells cultured on the SiO_2/β-TCP/POC and IBU-loaded SiO_2/β-TCP/POC were observed by phase contrast microscopy, shown in Figure 9. After being cultured for 3 d, the C2C12 cells grew well in polygonal or spindles shape, stretched sufficiently with their pseudopodia holding out and were affixed firmly to the surface of the cement. Higher cell density was found on the surface of the SiO_2/β-TCP/POC and IBU-loaded SiO_2/β-TCP/POC after 5 days' culture. This indicates IBU-loaded SiO_2/β-TCP/POC had no negative effect on cell morphology and viability.

Figure 10 is plotted the C2C12 cells morphology after being cultured with the leach liquor of IBU-loaded SiO_2/β-TCP/POC for 1 day. It is clear to see in Figure 9 a (200×) and Figure 9 a1 (600×) that the cytoskeleton and Factin fibers of C2C12 are stained in green and in integrated structure. Figure 9 b (200×) and Figure 9 b1 (600×) show the cell nucleus are evenly dyed in blue with integral nucleus DNA. The 3D visualization of the images (Figure 9 c (200×) and Figure 9 c1 (600×)) revealed that the cells spread well and the IBU-loaded SiO_2/β-TCP/POC scaffolds have good cell compatibility.

Table 2 Diameter of Inhibition Rings in *E. coli* cultures
(mm, x ±s, n = 3)

Species	SiO_2/β-TCP/POC	β-TCP/POC
1d	2.31 ± 0.81	7.56 ± 0.68
6d	12.72 ± 1.00	11.32 ± 1.57
18d	23.32± 3.15	14.07± 2.06

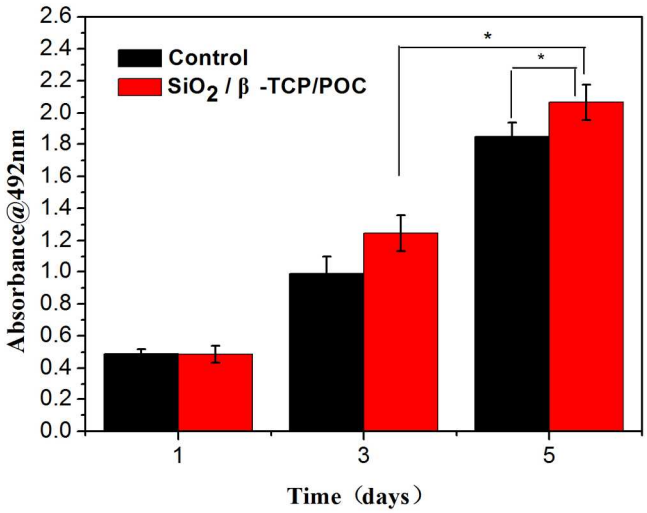

Figure 8.C2C12 cells proliferation on IBU-loaded SiO_2/β-TCP/POC scaffolds

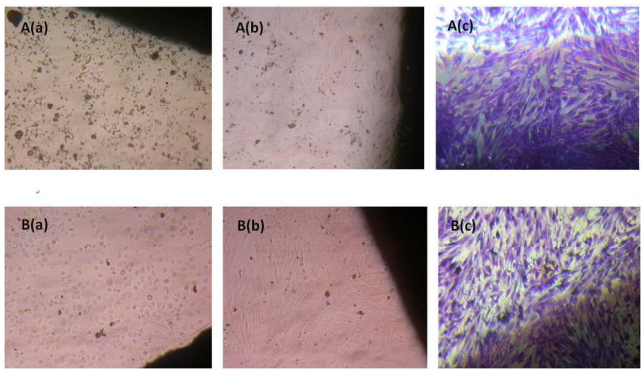

Figure 9 Microscope photos of C2C12 cells cultured on the SiO_2/β-TCP/POC (A) and IBU-loaded SiO_2/β-TCP/POC discs (B) after 1d (a) 3d (b) and 5d (c)

Discussion

Bone defect-related infections are still difficult to treat and present a challenge in clinic. The best treatment is to control infection and repair bone defect at the same time, which requires the bone graft composite having good antibacterial capability with sustained antibiotic release and also osteoinductivity.[25,26] Drug implants, such as bone cement with antibiotics, collagen sponge with gentamicin, polymeric carriers with various antibiotics, and silk carrier of antibiotics, are gaining increasing interest in treating infected bone defects[27-30] Although these carriers can deliver antibiotics locally to the infected bone and

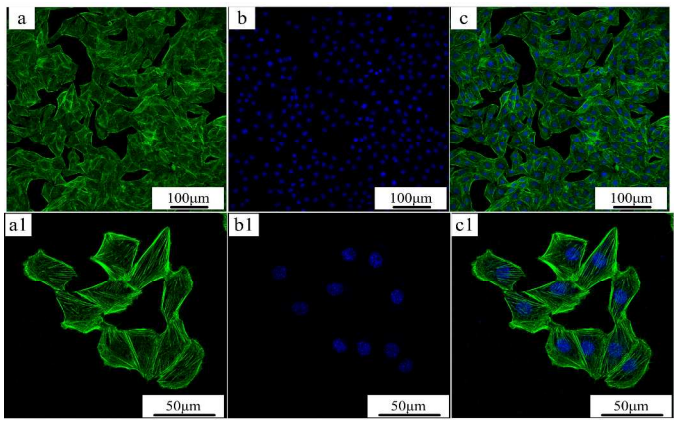

Figure 10. Observation of cytoskeleton stained with FITC Phalloidin (green) and nuclei stained with DAPI (blue) of C2C12 cells after 1 day coculture with leach liquor of IBU-loaded SiO_2/β-TCP/POC. (a-c ×200, a1-c1 ×600)

improve the treatment outcome, they still have a potential of inducing bacterial drug resistance and affect the bone recovery due to the monotonous drug releasing pattern and deficiency in bioactivity. Here, in this study, we first synthesis the hollow SiO_2 microsphere and loaded with IBU, and then fabricated hierarchically porous IBU-loaded SiO_2/β-TCP/POC complex scaffold through FFS-MDJ. The combination of the 3D printing techniques at room temperature and the hollow microsphere preparation is expected to bring the advantages of high osteogenetic activity and efficacious antimicrobial property.

An ideal scaffold for bone repair should possess appropriate architecture and properties for cell attachment, tissue ingrowth, and flow transport of nutrients and metabolic waste, among which an appropriate three-dimensional framework is a prerequisite [31]. To meet the demand of the porous structure, the IBU-loaded SiO_2/β-TCP/POC scaffolds utilized in present study exhibit mesoporous hollow structure with pore diameter of 3.65 nm (Figure 1) as well as the interconnected porous network, large pore sizes of 350–450μm (Figure 4). The macroporous of the scaffold was directly printed by FFS-MDJ three-dimensional printing system, while the mesoporous structure was formed by the modified sol-gel method of SiO_2 microspheres. In addition, microporosity might be produced by the biodegradation of POC and β-TCP. According to the previous reports, a typical macroporosity as a pore diameter of at least 100 μm was known to be compulsory for cell penetration and vascularization of the ingrown tissue[32-34], and microporosity between 10 μm and 100 μm should promote ion and liquid diffusion [35, 36]. In addition, the mesopores facilitates the peptide adsorption and provides protein-rich surface for cell attachment, differentiation and migration to form new tissues [37]. Therefore, the developed IBU-loaded SiO_2/β-TCP/POC scaffolds are hierarchically porous, which might facilitate the biodegradability and improve the bioactivity of the scaffold due to the increased surface area.

Beside the hierarchically pore size, highly interconnected pore structure is required to offer sufficient space for cell growth and to increase the volume of the invasion of surrounding tissue [38]. Especially, good pore interconnectivity has benefits for vascular ingrowth into the scaffolds. [39] In this study, the IBU-loaded SiO_2/β-TCP/POC scaffolds are in complete interconnection. On one hand, the interspacing distance in the same layer was set to be 0.39 mm and the distance between two layers was 0.9 mm. On the other hand, the high viscosity of pre-POC as a binder during the printing process and the after-polymerization characteristics of POC prevented the scaffold from collapse and endowed the excellent formability to the scaffolds. The two above factors ensured the fully interconnected pore structure of IBU-loaded SiO_2/β-TCP/POC scaffolds.

Ideally bioactive biomaterials need to interact actively with cells and stimulate cells growth [39]. Apart from the pore size and interconnectivity, the components of the scaffold are also important factors for good cell compatibility. In this study, the C2C12 cells could proliferate in the leach liquor of the IBU-loaded SiO_2/β-TCP/POC scaffolds, as demonstrated by the MTT assay (Figure 8). Figure 9 indicated that the morphologies of C2C12 cells in direct contact with IBU-loaded SiO_2/β-TCP/POC scaffolds were normal. Furthermore, the observation of cell morphology by confocal laser scanning microscope in Figure 10 suggested that the cells kept good bioactivity after 24 h cultivation. Thus, the IBU-loaded SiO_2/β-TCP/POC scaffolds was bioactivity and cytocompatible, with no obvious negative effects on cellular viability.

Suitable mechanical properties are important for bone tissue scaffolds to withstand external stresses during tissue generation. In general, the macroporous geometry can contribute the new bone ingrowth while decrease the mechanical strength. [41] In this study, the SiO_2/β-TCP/POC scaffold has the compressive modulus of 52.29 ± 5.15 MPa, which is higher than that of human trabecular bone (in the range of 2–12 MPa) and the β-TCP/POC scaffold. It might be the following reasons which leaded to this: First, the fabrication by 3D printing make scaffold a more uniform and continuous pore structure than other traditional porous techniques, which improve the compressive modulus. It is in line with the report that a uniform and continuous pore structure could improve the scaffold strength greatly. [42] Second, the addition of hollow SiO_2 microspheres in the scaffold might play the role of particulate reinforcement.

In general, biomaterials with local drug delivery properties are useful for bone regeneration, because implantation always leads to inflammatory responses. [43] Mesoporous biomaterials are favorable for the high loading and sustained release of drug due to their mesoporous channels. [44-46] In this study, IBU was chosen as a model drug because of its good anti-inflammatory effect and its suitable molecule size of about 1.0-0.6 nm.[47] Figure 7 shows the different IBU release behaviors of IBU-loaded SiO_2/β-TCP/POC and IBU loaded β-TCP/POC scaffolds. A burst release at the early stage was observed in the IBU loaded β-TCP/POC scaffold, and followed by continuous release at a

higher rate. For SiO_2/β-TCP/POC, IBU was released at a lower rate and initial release amount. In addition, the SiO_2/β-TCP/POC scaffold possessed a higher cumulative release amount than that of β-TCP/POC scaffold. It has been reported that the burst effect was decreased with the entrapment of drug in microspheres. [48] For SiO_2/β-TCP/POC scaffold, IBU was first gradually released from the hollow SiO_2 microspheres with the aid of mesoporous structure, and then released from the scaffold by the macropore, degradation and swelling degree of the scaffold. Therefore, the resulting SiO_2/β-TCP/POC scaffold exhibited controlled release of IBU by the hierarchical structure and modifying the composition of scaffolds.

The SiO_2/β-TCP/POC scaffold had sustained release of IBU in 18 days that gave the scaffold a long-term antibiotic activity (Table 2), which was probably related to the interconnected three-dimensional pore structure, high porosity and appropriate degradation rate. In the ongoing studies, the antibiotic mechanism of IBU and effectiveness of the IBU-loaded SiO_2/β-TCP/POC scaffold in the treatment of S. aureus induced bone defects will be further investigated.

Conclusions

A novel IBU-loaded SiO_2/β-TCP/POC scaffold was printed directly by FFS-MDJ, and IBU was loaded in the hollow SiO_2 microspheres to obtain a drug controllable release delivery in the repair of infected bone defects. The developed IBU-loaded SiO_2/β-TCP/POC scaffold presented hierarchically macro/mesoporous, highly interconnected pore structure, proper compressive modulus and biocompatibility. Moreover, the addition of hollow SiO_2microspheres were found to decrease the burst release and increase the cumulative release amount of IBU. In addition, the IBU-loaded SiO_2/β-TCP/POC showed a long-term effect on inhibiting *E. coli* growth by agar diffusion. These findings suggest that the IBU-loaded SiO_2/β-TCP/POC scaffold was promising in terms of its the hierarchically macro/mesoporous, highly interconnected pore structure and effective antimicrobial property, and may find potential applications for infected bone repair.

Acknowledgements

This investigation was supported by the National Basic Research Program of China (973 Program : 2012CB933600), National Natural Science Foundation of China (No.31370960, No. 31100678) and the 111 Project (B14018).

Notes and references

[1] S.Z. Ewa,S. Magdalena and B.L. Marta, *Mater Sci Forum*, 2013, **730**, 38-43.

[2] J. Yang , A.R. Webb and G.A. Ameer, *Adv Mater*, 2004, **16**, 511-516.

[3] C.J. Bettinger, *Macromolecular Bioscience*, 2011, **11**, 467-482.

[4] B. Kevin, J.P. Ball, C. Zdravka, R.A. Hoshi, G.A. Ameer and J.B. Allen, *Biomater Sci*, 2014, **2**, 1355-1366.

[5] S. Aydemir, A.D. Umran, E.A. Aksoy and V.H. Hasirci, *J Appl Polym Sci*, 2014, **131**(8).

[6] H. Aubin , J. W. Nichol , C. B. Hutson , H. Bae , A. L. Sieminski, D. M. Cropek , P. Akhyari and A. Khademhosseini , *Biomaterials,* 2010 , **31** , 6941.

[7] B. Piyush , R.M. Schweller, A. Khademhosseini, J.L. West and R. Bashir , *Annu Rev Biomed Eng,* 2014,**16**, 247-276 .

[8] S.P. Callahan , J.H. Callahan, C.E. Scheldegger and C.T. Silva , *Comput Sci Eng.*, 2008, **10**, 88-91.

[9] Y.P. Chen and M.D. Yang , *Appl MechanMater*, 2014,**670**, 936-941.

[10] V. Mourino, A. R. Boccaccini, *J. R. Soc. Interface*, 2010, **7**, 209.

[11] P.Zhao, D.W. Fei, F. Yang, *J Mater Chem B*, 2015, 3, 6885.

[12] S. Bettini, V. Bonfrate, *Biomacromolecules*, 2015, **16,** 2599-2608

[13] T.M. Allen and P.R. Cullis , *Science*, 2004, **303**, 1818-1822.

[14] Y. Yang , X. Guo, K.W. Wei , L.J. Wang , D.D. Yang, L.F. Lai, M.L. Cheng and Q. Liu, *J Nano part Res*, 2014, **16**(1), 1-10.

[15] Y. Nagai , L.D. Unsworth, S. Koutsopoulos and S.G. Zhang, *J. Control. Release,* 2006,**15**, 18-25.

[16] K. Sumaru and T. Kanamori, *Biochem. Eng. J.*, 2004, **20**, 127-136.

[17] M. Todo, N. Yamada, T. Arahira, Y. Ayukawa and K. Koyano, *IFMBE Proceedings,* 2014,**43**, 722-725.

[18] Y. Chen , H.R. Chen , D.P. Zeng , Y.B. Tian , F. Chen , J.W. Feng and J.L. Shi , *ACS Nano*, 2010,**4**, 6001-6013.

[19] J. Yang , D. Motlagh, A.R. Webb and G.A. Ameer , *Tissue Eng.*, 2005, **11,** 1876-1886.

[20] I. Djordjevic , N.R. Choudhury , N.K. Dutta and S. Kumar , *Polymer*, 2009, **50**, 1682-1691.

[21] L. Gao, C.D. Li, F.P. Chen and C.S Liu, *Biomed. Mater.,* 2015,**10**(3):035009.

[22] D. Das , Y. Yang, J.S. O'Brien, Dr. Breznan, S. Nimesh, S. Bernatchez , M. Hill , A. Sayari , R. Vincent and P. Kumarathasan , *J. Nanomater.*, 2014, **2014**(7), 731-747.

[23] S.H. Lee , J. Park , D.W. Kwon and T.H. Yoon , *B. Kor Chem. Soc.,* 2014,**35**, 1933-1938.

[24] T. Amna, H.M. Shamshi and M.S. Khil , *Ceram. Int.,* 2014,**40**,14305-14311.

[25] Y. Zhou, D. W. Hutmacher, S. L. Varawan and T. M. Lim, *composites Polym Int*. 2007, **56**, 333-42.

[26] K. Rezwan , Q. Z. Chen, J. J. Blaker and A. R. Boccaccini, *Biomaterials*, 2006, **27**, 3413-31.

[27] A. Jason Zana., M. Schwarz Edward, L. Kates Stephen and H. Awad, *Biomaterials*, 2016, **81**: 58-71.

[28] Q. Li and J. Coleman Nichola, *Dent. Mater. J*, 2014, **33**(6), 805-810.

[29] M. Pritchard Eleanor, T. Valentin, B.Panilaitis, F. Omenetto and D.Kaplan, *Adv. Funct. Mater.*, 2013, **23**(7), 854-861.

[30] D. Schneider Oliver, S. Loher, J. Brunner Tobias, P. Schmidlin and J. Stark Wendelin, *J Mater Chem.,* 2008, **18**(23), 2679-2684.

[31] C.L. Dai, H. Guo, J.X. Lu, J.L. Shi and J. Wei, *Biomaterials,* 2011, **32** (2011), 8506-8517.
[32] T.H. Kim, S.H. Oh and E.B. Kwon, *Macromol. Res*., 2013, **21**(8): 878-885
[33] S. Levenberg and R. Langer. *Curr Top Dev Biol*, 2004, **61**, 113-34.
[34] P.G. Duan, Z. Pan and L. Cao , *J Biomed Mater Res A,* 2013, **102(1)**:180–192
[35] B.D. Boyan, T.W. Hummert, D.D. Dean and Z. Schwartz, *Biomaterials* , 1996, **17**, 137-46.
[36] L.M. Mathieu, T.L. Mueller, P.E. Bourban, D.P. Pioletti, R. Müller and J.A. Månson, *Biomaterials,* 2006, **27**(6), 905-16.
[37] T.J. Webster, R.W. Siegel and R. Bizios, *Biomaterials*, 1999, **20**(13), 1221-7.
[38] J. Wei, F.P. Chen, J. W. Shin, H. Hong, C.L. Dai and J.C. Su, *Biomaterials*, 2009, **30**, 1080–1088.
[39] E.C. Novosel, C. Kleinhansand P.J. Kluge,*Adv Drug Deliv Rev,* 2011,**63,**300-11.
[40] X.Y. Zhao , L. Sun , M.Z. Wang , Z.Y. Sun and J. Xie , *Polymer International,* 2014,**63**, 393-401.
[41] O. Richart , M. Descamps and A. Liebetrau , *Engineering Materials*, 2001, **192**, 425-428.
[42] C. Wu, Y. Luo, G. Cuniberti, Y. Xiao and M. Gelinsky, *Acta Biomater*, 2011, **7**, 2644-50.
[43] J.H. Zhang, S.C. Zhao, Y.F. Zhu, Y.J. Huang , M. Zhu and C.L. Tao, *Acta Biomater*, 2014, **10**(5), 2269–2281.
[44] Y.L. Hong, X.S. Chen, X.B. Jing, H.S. Fan, Z.W. Gu and X.D. Zhang, *Adv Funct Mater*, 2010, **20**, 1503–10.
[45] G.Z. Jin, E. Mohamed and H.W. Kim, *RSC Adv*., 2015, **5**, 26832–26842.
[46] M. Zhu, J.L. Shi, Q.J. He, L.X. Zhang, F. Chen and Y. Chen, *J Mater Sci*., 2012, **47**, 2256–63.
[47] S.L. Guevara-Fernandezde, C.V. Ragel and M. Vallet-Regi, *Biomater.*, 2003, **4**,4037-43.
[48] U.A. Sezer, D. Arslantunali, E.A. Aksoy, V. Hasirci and N. Hasirci, *J. App. Polym. Sci.,* 2014,**131**, 40110.

Graphical abstract

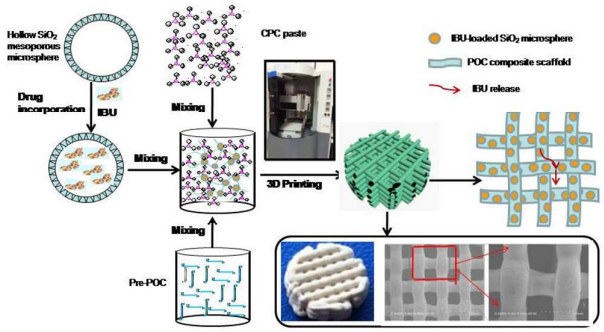

Figure Illustration of the hierarchically porous IBU-loaded SiO_2/β-TCP/POC scaffold